Supplementary material

1. Method

1.1 Synthesis of Cy7-labeled COS (COS-Cy7)

Synthesis was performed as previously described with some minor modifications[1]. COS (100 mg) was dissolved in 8 mL distilled water; the pH of the reaction solution was adjusted to 9.0 (using 0.5 M NaOH). Cy7-NHS ester (1 mg/mL) initially dissolved in 1 mL distilled water was added to a stirred solution of COS. The reaction mixture was stirred magnetically for 12 h (in the dark) at room temperature. The obtained mixture was lyophilized and then washed with 5 mL DMSO. After every run of wash, the mixture was centrifuged (for 10 min at 10000 rpm) to remove the unreacted Cy7-NHS; washing repeated 10 times. Finally, the purified COS-Cy7 was reconstituted in approximately 200 μL distilled water and lyophilized.

1.2 Physiochemical characterization

COS-Cy7 (0.1 μg/mL) was analyzed by Time-of-Flight-Mass Spectrometer (TOF6600-MS4500, Agilent, USA). Briefly, COS-Cy7 powder was dissolved in distilled water, and a small aliquot (1 mL) was used for analysis by TOF-MS. The mobile phase was a mixture of methanol and distilled water (80/20, *v/v*). To verify the chemical structure of COS and COS-Cy7, Fourier transforms infrared spectroscopy (FT-IR) spectra were recorded on a PerkinElmer Spectrum™ (Specrum 100). KBr method was adopted for testing sample preparation. The absorption and fluorescence spectra of COS-Cy7 and Cy7-NHS were recorded with Infinite M200 microplate reader

(TECAN, Switzerland).

2. Results

2.1 Synthesis and characterization of COS-Cy7

COS used in the present study was analyzed as previously reported [2]. COS-Cy7 was synthesized via a one-step protocol (Fig. S1). COS was labeled with Cy7-NHS ester by acylating their primary amines. COS-Cy7 was obtained as a solid powder after freeze-drying. The chemical structures of COS and COS-Cy7 were characterized by FT-IR. The FT-IR spectra of COS (Fig. S2A) showed basic characteristic absorption peaks at 1080 cm^{-1} (C-O stretching vibration of 3-OH) and 1623 cm^{-1} (-NH2). On the other hand, the characteristic band at 1623 cm^{-1} was disappeared in the FT-IR spectrum of COS-Cy7 (Fig. S2A), indicating amidation of NH_2 of COS. Furthermore, multiple characteristic peaks at approximately 2400 cm^{-1} (attributed to N-H stretching vibration in secondary amine) revealed the acylation of COS. Peaks higher than 1000 in TOF-MS results also confirmed the synthesis of COS-Cy7 (Fig. S3).

UV-vis spectrum analysis showed that COS-Cy7 had an absorbance peak at a wavelength of 748 nm and conjugated ~1.2 nmol of Cy7 per 1 mg of COS (Fig. S2B). COS-Cy7 and Cy7-NHS almost have the same pattern of UV-vis. This is because that both of them have the same fluorescence emission and excitation spectrum, as measured by fluorescence spectrophotometer (Fig. S2C and S2D). These results imply that chemical conjugation of Cy7 to COS does not affect the emission and excitation spectrum of Cy7-NHS.

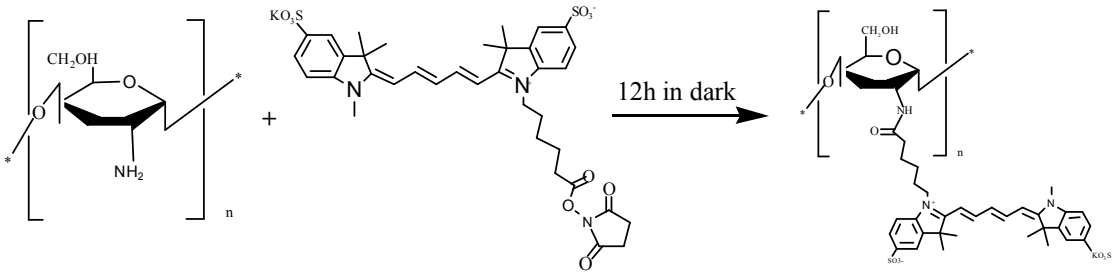

Fig. S1 Synthesis formula of COS-Cy7

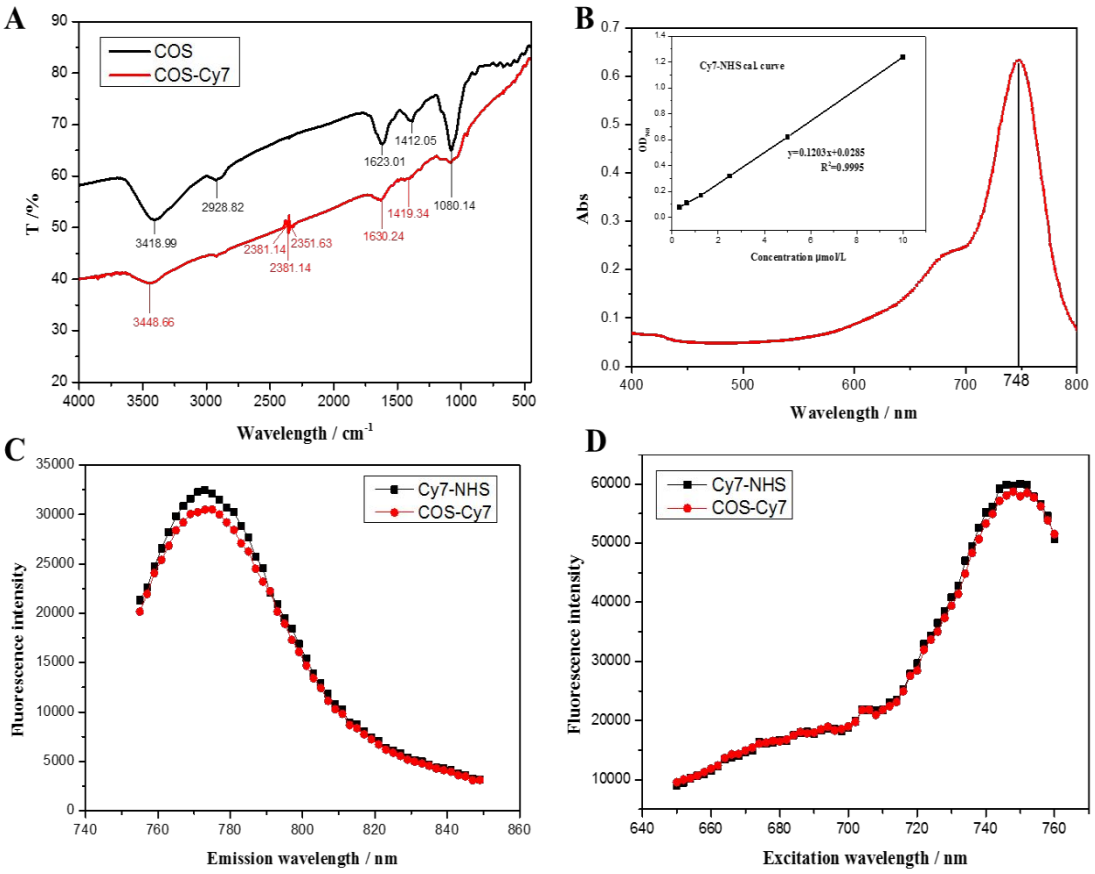

Fig.S2 Characterization of COS-Cy7. (A) FT-IR spectra of COS and COS-Cy7. (B) UV-vis spectrum of COS-Cy7. (C) Fluorescence spectrum of COS-Cy7 and Cy7-NHS at an excitation wavelength of 725 nm. (D) Fluorescence spectrum of COS-Cy7 and Cy7-NHS at an emission wavelength of 795 nm

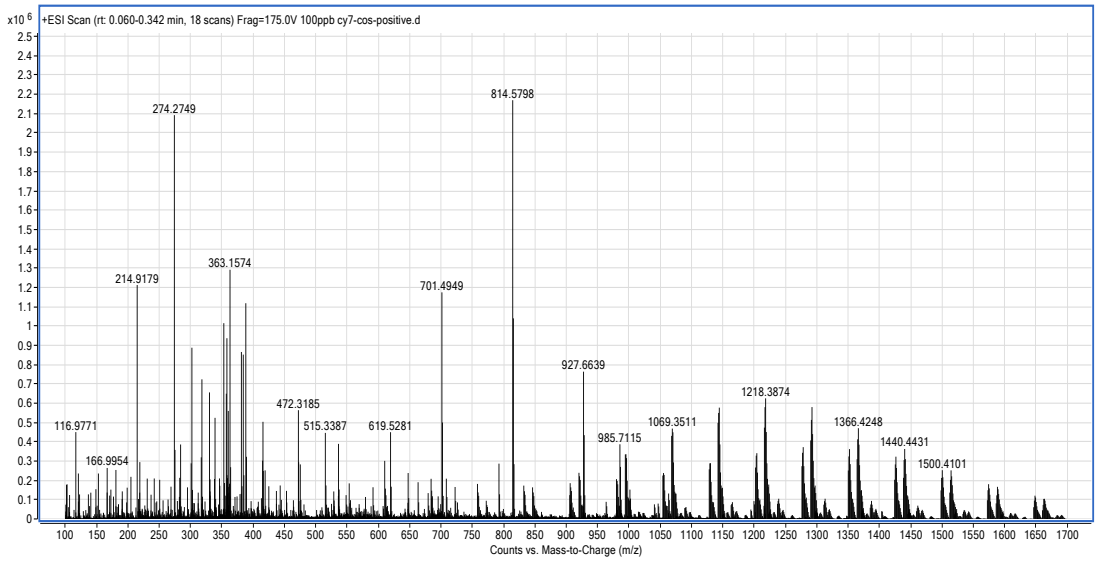

Fig. S3 MALDI-TOF-MS image of COS-Cy7

Table S1 Basic information of commercial chitosan for chitosan oligosaccharide preparation.

Project	Standards
Appearance	Off white powder
Deacetylation	≥90%
pH	7-8
Loss on drying	≤8%
Ignition Residue	≤0.5%
Undissolved Substance	≤1%
Particle Size	200 mpa.s
Heavy Metal	≤10 ppm
Arsenic	≤0.5 ppm
Particle Size	40-100 mesh
Yeast & Mould	≤ 10 cfu/g
Total Plate Counts	≤ 1000 cfu/g

Table S2 Primers used for qRT-PCR.

Gene names	Primers
β-actin	Forward 5'-GAAGATCAAGATCATTGCTCCTC-3'
	Reverse 5'-ATCCACATCTGCTGGAAGG-3'
HMOX1	Forward 5'-GAACTTTCAGAAGGGCCAG-3'
	Reverse 5'-TAGATGTGGTACAGGGAGG-3'
GCLM	Forward 5'-GTTGACATGGCCTGTTCAG-3'
	Reverse 5'-AACTCCATCTTCAATAGGAGGT-3'
SLC7A11	Forward 5'-CATCGTCCTTTCAAGGTGC-3'
	Reverse 5'-ATAGAGGGAAAGGGCAACC-3'
Nrf2	Forward 5'-AGGTTGCCCACATTCCCAAA-3'
	Reverse 5'-ACGTAGCCGAAGAAACCTCA-3'

Table S3 Flow cytometry analysis of KCC853 after COS treatment.

Group	Apoptosis state (%)				Cell cycle distribution (%)		
	Live	Early apoptosis	Late apoptosis	Dead	G0/G1	G2/M	S
Control	91.15 ±0.04	2.52 ± 0.34	3.34 ± 0.06	3.00 ± 0.36	67.91 ± 5.61	8.76 ± 1.62	23.32 ±2.48
COS-250	91.30 ±0.28	3.33 ± 0.52	4.15 ± 0.19	1.23 ± 0.05	68.70 ± 3.12	9.18 ± 0.65	22.12 ±1.06
COS-500	83.81 ±0.64	6.96 ± 0.11	7.70 ± 0.49	1.55 ± 0.05	64.40 ± 4.50	7.42 ± 1.97	28.14 ±2.35
COS-1000	26.77 ±0.21	55.05 ± 0.91	15.11 ± 0.27	3.07 ± 0.96	43.07 ± 2.67	25.35 ±1.66	31.58 ±2.11

Table S4 Biomarkers in serum of liver and kidney function of mice that received the different treatment.

	BUN	Cr	AKP	ALT	AST	ALB
Control	8.73±1.63	11.25±4.13	57.13±11.76	35.13±7.92	138.38±25.88	24.83±1.57
COS 10	6.86±0.94	10.38±1.19	65.13±17.26	37.25±12.07	121.13±29.02	26.48±2.10
COS 20	8.97±0.94	12.29±0.95	62.00±19.32	43.00±18.73	168.43±35.24	25.66±1.07
COS 40	8.67±1.66	9.67±1.63	65.00±15.58	38.17±22.59	105.67±25.90	27.32±1.22

References

[1] Li, J., Jiang, B., Lin, C., Zhuang, Z., Fluorescence tomographic imaging of sentinel lymph node using near-infrared emitting bioreducible dextran nanogels. *International Journal of Nanomedicine* 2014, *9*, 5667-5682.

[2] Zhai, X., Yang, X., Zou, P., Shao, Y*., et al.*, Protective Effect of Chitosan Oligosaccharides Against Cyclophosphamide-Induced Immunosuppression and Irradiation Injury in Mice. *Journal of food science* 2018, *83*, 535-542.